Pramana – J. Phys. (2020) 94:147
https://doi.org/10.1007/s12043-020-02022-8

Some Bianchi I dark energy models in Brans–Dicke theory

G P SINGH[1],*, ASHWINI R LALKE[1] and NIKHIL HULKE[2]

[1]Department of Mathematics, Visvesvaraya National Institute of Technology, Nagpur 440 010, India
[2]Department of Applied Mathematics, Shri Ramdeobaba College of Engineering and Management, Nagpur 440 013, India
*Corresponding author. E-mail: gps.math2015@gmail.com; gpsingh@mth.vnit.ac.in

MS received 7 February 2020; revised 28 July 2020; accepted 7 August 2020

Abstract. The present article deals with the study of interacting and non-interacting dark energy (DE) and dark matter (DM) in the spatially homogeneous and anisotropic Bianchi I space–time within the framework of Brans–Dicke (BD) scalar–tensor theory of gravitation. As the set of field equations is not closed, exact solutions are obtained using power-law relation and assuming a linearly varying deceleration parameter. The physical acceptability and stability of the obtained model are scrutinised using energy conditions and squared speed of sound. The statefinder diagnostic method is adopted to discuss and measure the deviation of the considered model from the Λ cold dark matter (ΛCDM) model.

Keywords. Bianchi I Universe; Brans–Dicke theory; linearly varying deceleration parameter; dark energy.

PACS Nos 98.80.–k; 95.36.+x

1. Introduction

The observations of type Ia Supernovae (SNe Ia) [1–3] together with measurements of the cosmic microwave background (CMB) [4] and galaxy power spectrum [5] suggested that we live in the Universe which is experiencing an accelerating phase of expansion. The common property of the inflationary and late-time stages of our Universe is the stage of accelerated expansion. An exotic fluid dominates such a Universe with negative pressure called dark energy (DE), which constitutes approximately 2/3 of the Universe. Wilkinson microwave anisotropy probe (WMAP) satellite [4,6,7] experiment showed that the Universe is composed of 73% DE, 22% non-baryonic (relativistic) dark matter (DM) and the rest 5% usual baryonic matter as well as radiation. Many theoretical models in various literature have investigated the behaviour of DE. Moreover, for explaining the current accelerating Universe, several cosmological models have been proposed, which are on scalar field models, modified gravity, inhomogeneous models, and many more.

The equation of state (EoS) parameter, $\gamma(t)$, is defined as $\gamma(t) = p/\rho$, where p is the pressure and ρ is the energy density, which characterised that the DE model is not always constant. From a theoretical point of view, through the EoS parameter, one can study the nature of DE. EoS can either be considered variable [8–10] or constant [11,12], where $\gamma = -1$ is for vacuum fluid, 0 for dust fluid, $+1/3$ for radiation and $+1$ for the stiff dominated Universe. Sahni and Starobinsky [13] have developed a technique for the regeneration of EoS in their investigation from the experimental data. The most excellent way to solve the coincidence problem in cosmology is by assuming that there is a small transfer of energy between DE and DM [14,15]. At present, such an energy flow explains the energy densities of DE and DM, which are almost equal.

A class of Bianchi-type space–time geometry plays an integral part in understanding the evolution and studying possible effects of anisotropy in the early stages of the Universe. Bali [16,17] and Kao and Lin [18] have investigated Bianchi I model in a different context of gravity. Recently, Raushan *et al* [19] have examined locally rotationally symmetric (LRS) Bianchi I model which is filled with a bulk viscous fluid within the framework of $f(R)$ gravity.

The Brans–Dicke (BD) theory [20], an alternative or an extension of Einstein's theory of general relativity, is the most prominent scalar–tensor theory of gravitation. It comprises a massless scalar field ϕ, a dimensionless BD coupling parameter ω and gravitational constant G

Published online: 13 October 2020

that is replaced with the reciprocal of a scalar field ϕ. Several limits on the BD coupling parameter ω were obtained after the release of the WMAP data report on CMB anisotropy. Large values of ω imply the tensor part, whereas small values of ω imply a contribution from the scalar field. The BD theory reduces to the general theory of relativity (GR) when ϕ = constant and $\omega \to \infty$ [21,22]. However, Romero and Barros [23] have pointed out that in the case of an exact solution when $\omega \to \infty$ then BD theory does not always yield GR. Furthermore, this theory furnishes suitable solutions to several cosmological issues; some of these are Universe inflation and late-time behaviour, cosmic acceleration and coincidence problem. More interestingly, the theory can cause cosmic acceleration even without the quintessence field in the matter-dominated era [24]. Many researchers have investigated several aspects of BD cosmology [25–27]. Singh and Rai [28] have discussed the foundation and prospects of scalar–tensor theory of gravity.

Several researchers proposed the interacting scenario of DE cosmological models [29–35]. The interacting and non-interacting scenario for DE and DM are studied in [36–39]. Motivated by the above studies on interacting and non-interacting cosmological models in BD theory, in this paper, we study the interacting and non-interacting DE and DM in spatially homogeneous and anisotropic Bianchi I model in the BD theory of gravitation. To get a deterministic solution of the field equation, we have assumed two physically plausible relations: (1) power-law relation between the scalar field and the scale factor and (2) the linearly varying deceleration parameter (LVDP). Both the cases of interacting and non-interacting DE scenarios were considered, and the results obtained. Physical acceptance and stability of the considered models are checked using energy conditions and squared speed of sound. The anisotropy parameter and statefinder diagnostic pair are also analysed.

The paper is organised as follows: Section 2 deals with the field equations and their solutions. Sections 3 and 4 investigate the non-interacting and interacting DE and DM, respectively. The graphical behaviour of EoS parameters, density parameters, energy conditions and squared speed of speed are discussed in brief for non-interacting and interacting DE and DM models. The analysis of the anisotropy parameter is given in §5. Section 6 gives statefinder diagnostic and §7 gives a concise conclusion of the study.

2. Field equations and solutions

The homogeneous and anisotropic Bianchi I Universe is given as

$$ds^2 = A^2\,dx^2 + B^2\,dy^2 + C^2\,dz^2 - dt^2, \tag{1}$$

where metric potentials A, B and C are the functions of time t alone. We work in units where $\hbar = K_B = c = 8\pi G_0 = 1$, where G_0 is the current value of G. The BD [20,40,41] field equations for the combined scalar and tensor fields are given by

$$R_{ij} - \frac{1}{2}Rg_{ij} - \omega\phi^{-2}\left(\phi_{,i}\phi_{,j} - \frac{1}{2}g_{ij}\phi^{,k}\phi_{,k}\right) - \phi^{-1}(\phi_{i;j} - g_{ij}\phi^{,k}_{;k}) = \phi^{-1}(T_{ij}), \tag{2}$$

where R is the Ricci scalar, R_{ij} is the Ricci tensor, T_{ij} is the energy–momentum tensor and the scalar field ϕ satisfies equation

$$\phi^{,k}_{;k} = \frac{T^i_j}{3+2\omega}. \tag{3}$$

The EoS parameters of DM and DE are given by

$$\gamma_m = \frac{p_m}{\rho_m} \quad \text{and} \quad \gamma_{de} = \frac{p_{de}}{\rho_{de}}, \tag{4}$$

where p_m and p_{de} are the pressure and ρ_m and ρ_{de} are the energy densities of DM and DE, respectively. We denote $T^i_{j(m)}$ and $T^i_{j(de)}$ as energy–momentum tensors of DM and DE which are given by

$$T^i_{j(m)} = \text{diag}[-\rho_m, p_m, p_m, p_m,] = \text{diag}[-1, \gamma_m, \gamma_m, \gamma_m]\rho_m, \tag{5}$$

$$T^i_{j(de)} = \text{diag}[-\rho_{de}, p_{de}, p_{de}, p_{de},] = \text{diag}[-1, \gamma_{de}, \gamma_{de}, \gamma_{de}]\rho_{de}. \tag{6}$$

So, the energy–momentum tensor is given by

$$T^i_j = T^i_{j(m)} + T^i_{j(de)}. \tag{7}$$

The field equations (2) and (3) for metric (1) in the co-moving coordinate system subsequently lead to the following system of equations:

$$\frac{\dot{A}\dot{B}}{AB} + \frac{\dot{B}\dot{C}}{BC} + \frac{\dot{A}\dot{C}}{AC} - \frac{\omega}{2}\frac{\dot{\phi}^2}{\phi^2} + \left(\frac{\dot{A}}{A} + \frac{\dot{B}}{B} + \frac{\dot{C}}{C}\right)\frac{\dot{\phi}}{\phi} = \frac{\rho_m + \rho_{de}}{\phi}, \tag{8}$$

$$\frac{\ddot{B}}{B} + \frac{\ddot{C}}{C} + \frac{\dot{B}\dot{C}}{BC} + \frac{\omega}{2}\frac{\dot{\phi}^2}{\phi^2} + \frac{\ddot{\phi}}{\phi} + \left(\frac{\dot{B}}{B} + \frac{\dot{C}}{C}\right)\frac{\dot{\phi}}{\phi} = \frac{1}{\phi}\left(-\gamma_m\rho_m - \gamma_{de}\rho_{de}\right), \tag{9}$$

$$\frac{\ddot{A}}{A} + \frac{\ddot{C}}{C} + \frac{\dot{A}\dot{C}}{AC} + \frac{\omega}{2}\frac{\dot{\phi}^2}{\phi^2} + \frac{\ddot{\phi}}{\phi} + \left(\frac{\dot{A}}{A} + \frac{\dot{C}}{C}\right)\frac{\dot{\phi}}{\phi} = \frac{1}{\phi}\left(-\gamma_m\rho_m - \gamma_{de}\rho_{de}\right), \tag{10}$$

$$\frac{\ddot{A}}{A} + \frac{\ddot{B}}{B} + \frac{\dot{A}\dot{B}}{AB} + \frac{\omega}{2}\frac{\dot{\phi}^2}{\phi^2} + \frac{\ddot{\phi}}{\phi} + \left(\frac{\dot{A}}{A} + \frac{\dot{B}}{B}\right)\frac{\dot{\phi}}{\phi}$$

$$= \frac{1}{\phi}\left(-\gamma_m \rho_m - \gamma_{de}\rho_{de}\right), \tag{11}$$

$$\ddot{\phi} + \left(\frac{\dot{A}}{A} + \frac{\dot{B}}{B} + \frac{\dot{C}}{C}\right)\dot{\phi} = \frac{\rho_m(1-3\gamma_m) + \rho_{de}(1-3\gamma_{de})}{3+2\omega}. \tag{12}$$

Here 'overhead dot' denotes derivative with respect to time. The field equations (8)–(11) are a system of four linearly independent equations with six unknown parameters. Thus, we required two additional constraints relating to these parameters to obtain the system's explicit solutions. For solving the highly nonlinear BD field equations for the metric, we assume power-law relation [42] as

$$\phi = \alpha a^{\beta}, \tag{13}$$

which is a relation between the scalar field ϕ and average cosmic scale factor a, where α is any constant and β is a positive parameter. The reason behind choosing this ansatz is that it directly relates the strength of gravity with the scale factor a [43].

Secondly, we consider LVDP [44], which exhibits a phase transition from the early deceleration to current acceleration. Akarsu *et al* [49] studied the cosmological parameter of the LVDP Universe constrained with H(Z)+SNe Ia data points [45–48]. Their work suggested that LVDP is the only unbiased model of the Universe that ends with a big rip. The form of deceleration parameter that varies linearly with respect to time [44] is given as

$$q = -kt + m - 1, \tag{14}$$

which gives average scale factor a as

$$a = a_1 \exp\left(\frac{2}{m}\tanh^{-1}\left(\frac{kt}{m} - 1\right)\right), \tag{15}$$

where $k > 0$, $m > 0$ and a_1 is a constant. Akarsu and Dereli [44] in their work depict the graph of LVDP by choosing $k = 0.097$ and $m = 1.6$. They have also mentioned that these chosen values of k and m are consistent with the result obtained by the kinematics analysis of Cunha [47]. Following the values mentioned above, we have chosen the same values of free parameters k and m in such a way that q exhibits the transition phase from initial deceleration to late-time acceleration and is consistent with the recent observations [50]. Chaubey and Shukla [51] have examined the anisotropic models with the cosmological constant $\Lambda(t)$ in modified $f(R,T)$ theory considering the same LVDP. Here, the Hubble parameter of the Universe is obtained by using the above equation as

$$H = \frac{-2}{t(kt - 2m)}. \tag{16}$$

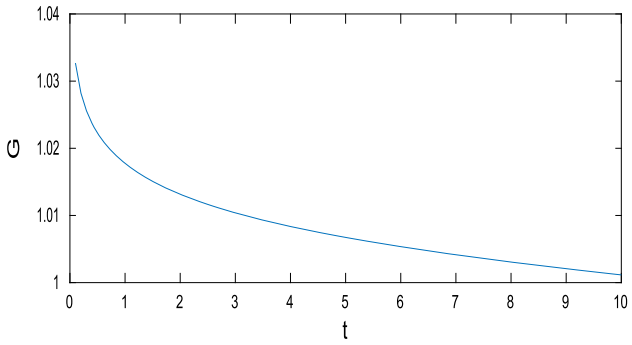

Figure 1. Evaluation of gravitational constant G as a function of cosmic time t for $k = 0.097$, $m = 1.6$ and $a_1 = 1.5$.

The variation of gravitational constant G decides the strength of gravity that is dominant on a large scale; that is why it is an interesting aspect from a cosmological point of view. The Newtonian gravitational constant in BD theory is expressed as

$$G = \frac{1}{\phi}.$$

Figure 1 illustrates the evaluation of G as a function of cosmic time. From the figure, it observed that G or $1/\phi$ is a decreasing function of cosmic time. This fact shows that ϕ is an increasing function of time. Assessment of the behaviour of quantity $\dot{G}/G$ yields time variation of Newtonian gravitational constant. Wu and Chen [52] have obtained the constraints on G's variance at the 2σ confidence level as

$$-1.75 \times 10^{-12}\,\mathrm{yr}^{-1} < \left(\frac{\dot{G}}{G}\right)_0 < 1.05 \times 10^{-12}\,\mathrm{yr}^{-1}.$$

In our model, the time variation of gravitational constant is $(\dot{G}/G) = -\beta H$. Thus, by the above two relations, in this case, we get

$$\left|\frac{\dot{G}}{G}\right|_0 = |\beta H_0| < 10^{-12}\,\mathrm{yr}^{-1}.$$

It implies,

$$|\beta| < \frac{10^{-12}}{H_0}\,\mathrm{yr}^{-1}.$$

Considering the best-fit value of $H_0 = 74.2\,\mathrm{km\,s^{-1}\,Mpc^{-1}} = 7.57 \times 10^{-11}\,\mathrm{yr}^{-1}$ [53], one can estimate the bounds on β as,

$$|\beta| < 0.0132.$$

Xu *et al* [54] have investigated the cosmic observational constraints on the holographic DE under the composition of BD theory and obtained the 1σ bound on β as

$\beta < 0.135807$. Furthermore, several researchers have analysed the cosmological observations to constrain the BD coupling parameter ω. In 2004, Acquaviva *et al* [55] used the Markov chain Monte Carlo approach with CMB data to obtain a constraint on ω as $\omega > 120$ at 2σ confidence level. However, with additional large-scale structure along with CMB data, Wu and Chen [52] showed the 2σ (95.5%) bound on ω as $\omega < -120$ or $\omega > 97.8$ in their work. Under the ranges mentioned above or limits of ω, it will be worthwhile to choose the enormous value of $|\omega|$ in this work.

Now, further, for solving field equations (9)–(11) for metric (1), we get

$$\frac{\ddot{A}}{A} - \frac{\ddot{B}}{B} + \left(\frac{\dot{C}}{C} + \frac{\dot{\phi}}{\phi}\right)\left(\frac{\dot{A}}{A} - \frac{\dot{B}}{B}\right) = 0, \tag{17}$$

$$\frac{\ddot{B}}{B} - \frac{\ddot{C}}{C} + \left(\frac{\dot{A}}{A} + \frac{\dot{\phi}}{\phi}\right)\left(\frac{\dot{B}}{B} - \frac{\dot{C}}{C}\right) = 0, \tag{18}$$

$$\frac{\ddot{A}}{A} - \frac{\ddot{C}}{C} + \left(\frac{\dot{B}}{B} + \frac{\dot{\phi}}{\phi}\right)\left(\frac{\dot{A}}{A} - \frac{\dot{C}}{C}\right) = 0. \tag{19}$$

Integrating eqs (17)–(19), we get

$$\frac{\dot{A}}{A} - \frac{\dot{B}}{B} = \frac{c_1}{ABC\phi}, \tag{20}$$

$$\frac{\dot{B}}{B} - \frac{\dot{C}}{C} = \frac{c_2}{ABC\phi}, \tag{21}$$

$$\frac{\dot{A}}{A} - \frac{\dot{C}}{C} = \frac{c_3}{ABC\phi}, \tag{22}$$

where c_1, c_2 and c_3 are constants of integration. Again integration of eqs (20)–(22) gives

$$\frac{A}{B} = d_1 \exp\left(c_1 \int \frac{\mathrm{d}t}{ABC\phi}\right), \tag{23}$$

$$\frac{B}{C} = d_2 \exp\left(c_2 \int \frac{\mathrm{d}t}{ABC\phi}\right), \tag{24}$$

$$\frac{C}{A} = d_3 \exp\left(c_3 \int \frac{\mathrm{d}t}{ABC\phi}\right), \tag{25}$$

where d_1, d_2 and d_3 are integration constants. Now, we can find all metric potentials from eqs (23)–(25) as follows:

$$A(t) = k_1 a \exp\left(b_1 \int \frac{\mathrm{d}t}{a^3\phi}\right), \tag{26}$$

$$B(t) = k_2 a \exp\left(b_2 \int \frac{\mathrm{d}t}{a^3\phi}\right), \tag{27}$$

$$C(t) = k_3 a \exp\left(b_3 \int \frac{\mathrm{d}t}{a^3\phi}\right), \tag{28}$$

where $k_1 = (d_1 d_3^{-1})^{1/3}$, $k_2 = (d_1^{-2} d_3^{-1})^{1/3}$, $k_3 = (d_1 d_3^2)^{1/3}$, $b_1 = (c_1 - c_3)/3$, $b_2 = -(2c_1 + c_3)/3$ and $b_3 = (c_1 + 2c_3)/3$. Now, substituting the values of A, B and C in eq. (8), we get

$$H^2 = \frac{\rho_m + \rho_{de}}{D\phi} + \frac{X a^{-6}\phi^{-2}}{D}, \tag{29}$$

where $X = -(b_1b_2 + b_2b_3 + b_1b_3)$ and $D = (3 + 3\beta - \frac{\beta^2\omega}{2})$.

3. Non-interacting dark energy and dark matter

In this section, we shall examine the behaviour of EoS parameter and density parameter for the interacting DE and DM. The law of energy conservation equation $T^{ij}_{;j} = 0$, i.e. $T^{ij(m)}_{;j} + T^{ij(de)}_{;j} = 0$ yields

$$\dot{\rho}_m + 3\frac{\dot{a}}{a}(1+\gamma_m)\rho_m + \dot{\rho}_{de} + 3\frac{\dot{a}}{a}(1+\gamma_{de})\rho_{de} = 0. \tag{30}$$

The two dark components can be written separately as

$$\dot{\rho}_m + 3\frac{\dot{a}}{a}(1+\gamma_m)\rho_m = 0, \tag{31}$$

$$\dot{\rho}_{de} + 3\frac{\dot{a}}{a}(1+\gamma_{de})\rho_{de} = 0. \tag{32}$$

Integrating eq. (31) and using scale factor from eq. (15), we get the energy density of DM as

$$\rho_m = \rho_{m_0} a_1^{-3(1+\gamma_m)} \times \exp\left(-\frac{6(1+\gamma_m)}{m}\tanh^{-1}\left(\frac{kt}{m} - 1\right)\right), \tag{33}$$

where ρ_{m_0} is an integrating constant. Using ρ_m from eq. (33) in eq. (29), we get

$$\rho_{de} = \left[D\alpha a_1^{\beta} \exp\left(\frac{2\beta}{m}\tanh^{-1}\left(\frac{kt}{m} - 1\right)\right) - 3\Omega_{m_0} a_1^{-3(1+\gamma_m)} \times \exp\left(-\frac{6(1+\gamma_m)}{m}\tanh^{-1}\left(\frac{kt}{m} - 1\right)\right)\right] \times \frac{4}{(kt^2 - 2mt)^2} - X\alpha^{-1} a_1^{-(\beta+6)} \times \exp\left(\frac{-2(\beta+6)}{m}\tanh^{-1}\left(\frac{kt}{m} - 1\right)\right), \tag{34}$$

where $X = -(b_1b_2 + b_2b_3 + b_1b_3)$, $D = (3 + 3\beta - \frac{\beta^2\omega}{2})$ and $\Omega_{m_0} = \rho_{m_0}/3H^2$ is the energy density parameter of DM. Here subscript 0 shows the present value of

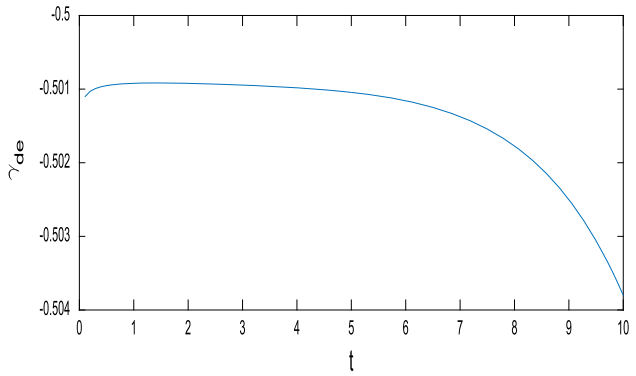

Figure 2. The plot of EoS parameter (γ_{de}) vs. cosmic time t of non-interacting model for $\alpha = 1$, $a_1 = 1.5$, $\beta = 0.01$, $k = 0.097$, $m = 1.6$, $\Omega_{m_0} = 0.3$, $\gamma_m = 0$, $M = -0.5$, $X = -1$ and $\omega = 1000$.

Ω_m. Now, EoS parameter of the DE can be obtained by using eqs (13), (33), (34) in eq. (9) as

$$\gamma_{de} = \frac{N}{D}, \tag{35}$$

where

$$\begin{aligned} N = &\Big[(\beta+2)(-kt+m-1) \\ &-\left(\beta^2\left(1+\frac{\omega}{2}\right)+\beta+1\right)\Big] \\ &\times\frac{4\alpha a_1^{\beta}}{(kt^2-2mt)^2}\exp\left(\frac{2\beta}{m}\tanh^{-1}\left(\frac{kt}{m}-1\right)\right) \\ &+M\alpha^{-1}\,a_1^{-(\beta+6)} \\ &\times\exp\left(\frac{-2(\beta+6)}{m}\tanh^{-1}\left(\frac{kt}{m}-1\right)\right) \\ &-\frac{12\gamma_m\Omega_{m_0}}{(kt^2-2mt)^2}a_1^{-3(1+\gamma_m)} \\ &\times\exp\left(-\frac{6(1+\gamma_m)}{m}\tanh^{-1}\left(\frac{kt}{m}-1\right)\right) \end{aligned}$$

and

$$\begin{aligned} D = &\left[D\alpha a_1^{\beta}\exp\left(\frac{2\beta}{m}\tanh^{-1}\left(\frac{kt}{m}-1\right)\right)\right. \\ &-3\Omega_{m_0}a_1^{-3(1+\gamma_m)} \\ &\left.\times\exp\left(-\frac{6(1+\gamma_m)}{m}\tanh^{-1}\left(\frac{kt}{m}-1\right)\right)\right] \\ &\times\frac{4}{(kt^2-2mt)^2}-X\alpha^{-1}a_1^{-(\beta+6)} \\ &\times\exp\left(\frac{-2(\beta+6)}{m}\tanh^{-1}\left(\frac{kt}{m}-1\right)\right), \end{aligned}$$

where $X = -(b_1b_2+b_2b_3+b_1b_3)$, $D = (3+3\beta-\beta^2\frac{\omega}{2})$ and $M = -(b_2^2+b_3^3+b_2b_3)$.

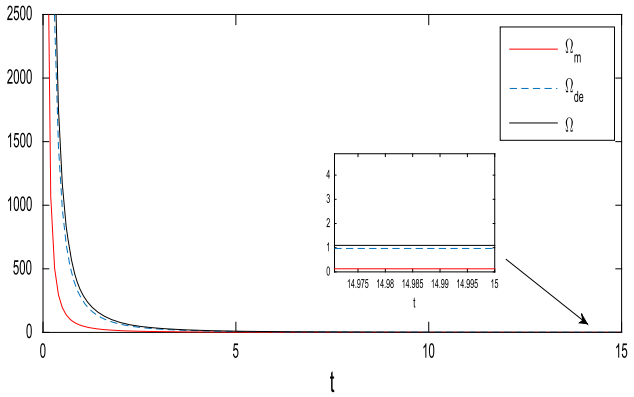

Figure 3. The plot of density parameter of DE and DM, and total density parameter (Ω) vs. cosmic time t of non-interacting model for $\alpha = 1$, $a_1 = 1.5$, $\beta = 0.01$, $k = 0.097$, $m = 1.6$, $\Omega_{m_0} = 0.3$, $\gamma_m = 0$, $M = -0.5$, $X = -1$ and $\omega = 1000$.

Figure 2 illustrates that the EoS parameter (γ_{de}) is entirely a negative valued function that evolves in the quintessence region. The expression for matter density parameter Ω_m is given by

$$\begin{aligned} \Omega_m &= \frac{\rho_m}{3H^2}, \\ \Omega_m &= \Omega_{m_0}a_1^{-3(1+\gamma_m)} \\ &\quad\times\exp\left(-\frac{6(1+\gamma_m)}{m}\tanh^{-1}\left(\frac{kt}{m}-1\right)\right). \end{aligned} \tag{36}$$

Similarly, DE density parameter Ω_{de} is given by

$$\begin{aligned} \Omega_{de} &= \frac{\rho_{de}}{3H^2}, \\ \Omega_{de} &= \frac{D\alpha}{3}a_1^{\beta}\exp\left(\frac{2\beta}{m}\tanh^{-1}\left(\frac{kt}{m}-1\right)\right) \\ &\quad-\frac{X\alpha^{-1}a_1^{-(\beta+6)}\exp\left(\frac{-2(\beta+6)}{m}\tanh^{-1}\left(\frac{kt}{m}-1\right)\right)}{12(kt^2-2mt)^{-2}} \\ &\quad-\Omega_{m_0}\,a_1^{-3(1+\gamma_m)} \\ &\quad\times\exp\left(-\frac{6(1+\gamma_m)}{m}\tanh^{-1}\left(\frac{kt}{m}-1\right)\right). \end{aligned} \tag{37}$$

Adding eqs (36) and (37) to obtain total density parameters Ω as

$$\begin{aligned} \Omega &= \Omega_m+\Omega_{de}, \\ \Omega &= \frac{D\alpha}{3}a_1^{\beta}\exp\left(\frac{2\beta}{m}\tanh^{-1}\left(\frac{kt}{m}-1\right)\right) \\ &\quad-\frac{X\alpha^{-1}a_1^{-(\beta+6)}\exp\left(\frac{-2(\beta+6)}{m}\tanh^{-1}\left(\frac{kt}{m}-1\right)\right)}{12(kt^2-2mt)^{-2}}. \end{aligned} \tag{38}$$

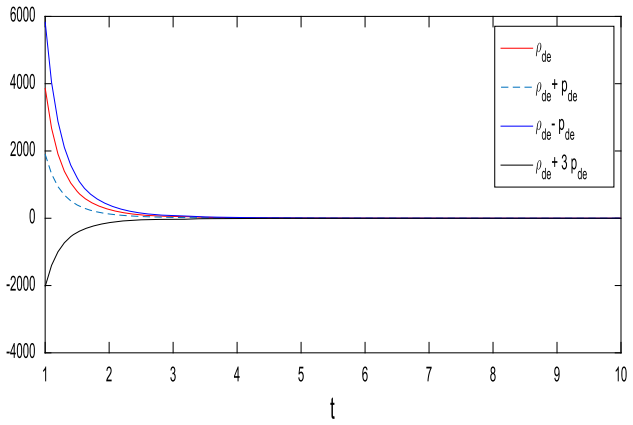

Figure 4. The plot of energy conditions vs. cosmic time t of the non-interacting model for $\alpha = 1$, $a_1 = 1.5$, $\beta = 0.01$, $k = 0.097$, $m = 1.6$, $\Omega_{m_0} = 0.3$, $\gamma_m = 0$, $M = -0.5$, $X = -1$ and $\omega = 1000$.

The variation of density parameters of DE and DM and Ω for cosmic time t is shown in figure 3. It is noticed that the plot of energy density parameter is slightly above the matter density parameter. More precisely, one can say that the value of the DE density parameter is greater than the matter density parameter. It is obvious from the figure that throughout the cosmic evolution, DE dominates the Universe. Moreover, it also observed that Ω tends asymptotically to 1 when time increases. Thus, the model predicts a flat Universe at late times as it is consistent with the recent observations suggested by the Planck satellite data report [50].

Figure 4 demonstrates that $\rho_{de} \geq 0$, $\rho_{de} \pm p_{de} \geq 0$ during the evolution of the Universe whereas $\rho_{de}+3p_{de}$ is negative at the beginning of the Universe and at late times, it approaches zero. For the considered model, squared speed of sound is given by

$$c_s^2 = \frac{\mathrm{d}p_{de}}{\mathrm{d}\rho_{de}}. \tag{39}$$

According to the fundamental principles of classical physical theories, the squared speed of sound should be non-negative, i.e., $c_s^2 \geq 0$, which induced the cosmological model to be stable; otherwise, it will be unstable classically against the background energy density's small perturbations [56]. More precisely, the adiabatic speed of sound for a stable model should be greater than or equal to zero (i.e., $c_s^2 \geq 0$), and for ensuring causality, it should be less than or equal to 1 (i.e., $c_s^2 \leq 1$). Figure 5 depicts that c_s^2 is within the range $0 \leq c_s^2 \leq 1$ as the Universe evolves.

4. Interacting dark energy and dark matter

In this section, we presume that there is an interaction between DE and DM. The positive quantity represented

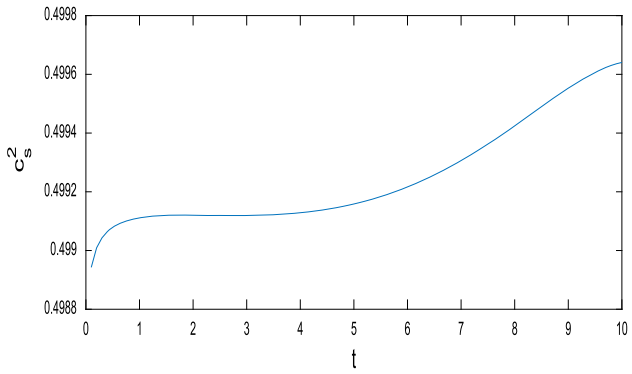

Figure 5. The plot of squared speed of sound vs. cosmic time t of the non-interacting model for $\alpha = 1$, $a_1 = 1.5$, $\beta = 0.01$, $k = 0.097$, $m = 1.6$, $\Omega_{m_0} = 0.3$, $\gamma_m = 0$, $M = -0.5$, $X = -1$ and $\omega = 1000$.

by

$$Q = 3H\sigma\rho_m, \tag{40}$$

gives the interaction between DE and DM [32,57], where σ is a coupling constant, which takes the value between -0.08 and 0.03 (95% CL) as per the recent observations proposed by Guo *et al* [57]. The energy conservation equation (30) can be expressed separately as

$$\dot{\rho}_m + 3\frac{\dot{a}}{a}(1+\gamma_m)\rho_m = Q, \tag{41}$$

$$\dot{\rho}_{de} + 3\frac{\dot{a}}{a}(1+\gamma_{de})\rho_{de} = -Q. \tag{42}$$

The second law of thermodynamics is fulfilled by considering interacting terms Q as positive to solve the coincidence problem [58]. Using the value of Q from eq. (40) in eq. (41) and then integrating, we obtain

$$\rho_m = \rho_{m_0} a^{-3(1+\gamma_m-\sigma)}. \tag{43}$$

From eq. (15), we get

$$\rho_m = \rho_{m_0} a_1^{-3(1+\gamma_m-\sigma)} \times \exp\left(-\frac{6(1+\gamma_m-\sigma)}{m}\tanh^{-1}\left(\frac{kt}{m}-1\right)\right), \tag{44}$$

where ρ_{m_0} is an integrating constant. Using eq. (15) in eq. (29), we get

$$\rho_{de} = \left[D\alpha a_1^{\beta}\exp\left(\frac{2\beta}{m}\tanh^{-1}\left(\frac{kt}{m}-1\right)\right) - 3\Omega_{m_0}a_1^{-3(1+\gamma_m-\sigma)} \times \exp\left(\frac{-6(1+\gamma_m-\sigma)}{m}\tanh^{-1}\left(\frac{kt}{m}-1\right)\right)\right] \times \frac{4}{(kt^2-2mt)^2} - X\alpha^{-1}a_1^{-(\beta+6)}$$

$$\times \exp\left(\frac{-2(\beta+6)}{m}\tanh^{-1}\left(\frac{kt}{m}-1\right)\right), \quad (45)$$

where $X = -(b_1b_2 + b_2b_3 + b_1b_3)$ and $D = (3 + 3\beta - \frac{\beta^2\omega}{2})$.

Using eqs (44) and (45) in eq. (9), we get the EoS parameter of DE as

$$\gamma_{de} = \frac{A}{B}, \quad (46)$$

where

$$\begin{aligned}A = &\Big[(\beta+2)(-kt+m-1)\\ &-\left(\beta^2\left(1+\frac{\omega}{2}\right)+\beta+1\right)\Big]\\ &\times\frac{4\alpha a_1^{\beta}}{(kt^2-2mt)^2}\exp\left(\frac{2\beta}{m}\tanh^{-1}\left(\frac{kt}{m}-1\right)\right)\\ &+M\alpha^{-1}a_1^{-(\beta+6)}\\ &\times\exp\left(\frac{-2(\beta+6)}{m}\tanh^{-1}\left(\frac{kt}{m}-1\right)\right)\\ &-\frac{12\gamma_m\Omega_{m_0}}{(kt^2-2mt)^2}a_1^{-3(1+\gamma_m-\sigma)}\\ &\times\exp\left(-\frac{6(1+\gamma_m-\sigma)}{m}\tanh^{-1}\left(\frac{kt}{m}-1\right)\right)\end{aligned}$$

and

$$\begin{aligned}B = &\left[D\alpha a_1^{\beta}\exp\left(\frac{2\beta}{m}\tanh^{-1}\left(\frac{kt}{m}-1\right)\right)\right.\\ &-3\Omega_{m_0}a_1^{-3(1+\gamma_m-\sigma)}\\ &\left.\times\exp\left(\frac{-6(1+\gamma_m-\sigma)}{m}\tanh^{-1}\left(\frac{kt}{m}-1\right)\right)\right]\\ &\times\frac{4}{(kt^2-2mt)^2}-X\alpha^{-1}a_1^{-(\beta+6)}\\ &\times\exp\left(\frac{-2(\beta+6)}{m}\tanh^{-1}\left(\frac{kt}{m}-1\right)\right).\end{aligned}$$

Here $X = -(b_1b_2+b_2b_3+b_1b_3)$, $D = (3+3\beta-\frac{\beta^2\omega}{2})$ and $M = -(b_2^2 + b_3^3 + b_2b_3)$.

The variation of γ_{de} vs. t for the interacting model is shown in figure 6. It observed that the plot of the EoS parameter of an interacting model for $\sigma = 0.02$ resembles that of the non-interacting model.

The matter density parameter Ω_m is given by

$$\begin{aligned}\Omega_m &= \frac{\rho_m}{3H^2},\\ \Omega_m &= \Omega_{m_0}a_1^{-3(1+\gamma_m-\sigma)}\\ &\quad\times\exp\left(-\frac{6(1+\gamma_m-\sigma)}{m}\tanh^{-1}\left(\frac{kt}{m}-1\right)\right).\end{aligned} \quad (47)$$

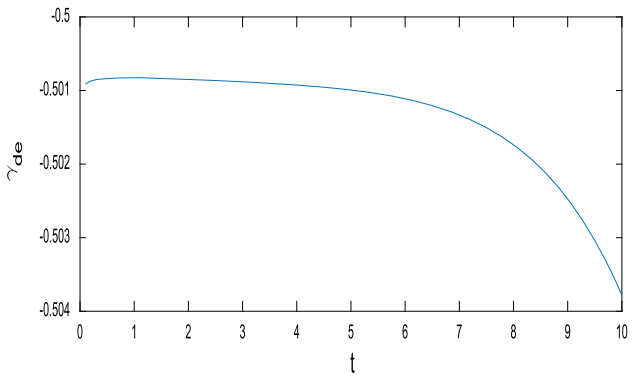

Figure 6. The plot of EoS parameter vs. cosmic time t of the interacting model for $\alpha = 1$, $a_1 = 1.5$, $\beta = 0.01$, $k = 0.097$, $m = 1.6$, $\Omega_{m_0} = 0.3$, $\gamma_m = 0$, $M = -0.5$, $X = -1$, $\omega = 1000$ and $\sigma = 0.02$.

Similarly, DE density parameter Ω_{de} is given by

$$\begin{aligned}\Omega_{de} &= \frac{\rho_{de}}{3H^2},\\ \Omega_{de} &= \frac{D\alpha}{3}a_1^{\beta}\exp\left(\frac{2\beta}{m}\tanh^{-1}\left(\frac{kt}{m}-1\right)\right)\\ &\quad-\frac{X\alpha^{-1}a_1^{-(\beta+6)}\exp\left(\frac{-2(\beta+6)}{m}\tanh^{-1}\left(\frac{kt}{m}-1\right)\right)}{12(kt^2-2mt)^{-2}}\\ &\quad-\Omega_{m_0}\,a_1^{-3(1+\gamma_m-\sigma)}\\ &\quad\times\exp\left(-\frac{6(1+\gamma_m-\sigma)}{m}\tanh^{-1}\left(\frac{kt}{m}-1\right)\right).\end{aligned} \quad (48)$$

Adding eqs (47) and (48), we obtain Ω as

$$\begin{aligned}\Omega &= \Omega_m + \Omega_{de},\\ \Omega &= \frac{D\alpha}{3}a_1^{\beta}\exp\left(\frac{2\beta}{m}\tanh^{-1}\left(\frac{kt}{m}-1\right)\right)\\ &\quad-\frac{X\alpha^{-1}a_1^{-(\beta+6)}\exp\left(\frac{-2(\beta+6)}{m}\tanh^{-1}\left(\frac{kt}{m}-1\right)\right)}{12(kt^2-2mt)^{-2}}.\end{aligned} \quad (49)$$

Figure 7 illustrates the plot of the density parameter of DE and DM and Ω as a function of t of the interacting model. It noticed that when time increases, Ω decreases and approaches asymptotically one at late times. Hence, one can say that the model predicts a flat Universe in the late epoch. It is also observed that the Universe is dominated by DE entirely for an interacting model.

Figure 8 shows that throughout the evolution of the Universe $\rho_{de} \geq 0$, $\rho_{de} \pm p_{de} \geq 0$ and $\rho_{de} + 3p_{de} \leq 0$. The squared speed of sound of the interacting model is given as

$$c_s^2 = \frac{\mathrm{d}p_{de}}{\mathrm{d}\rho_{de}}. \quad (50)$$

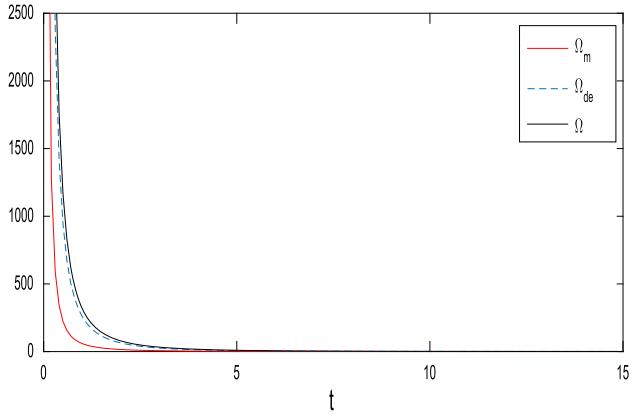

Figure 7. The plot of density parameter of DE and DM, and total density parameter (Ω) vs. cosmic time t of the interacting model for $\alpha = 1$, $a_1 = 1.5$, $\beta = 0.01$, $k = 0.097$, $m = 1.6$, $\Omega_{m_0} = 0.3$, $\gamma_m = 0$, $M = -0.5$, $X = -1$, $\omega = 1000$ and $\sigma = 0.02$.

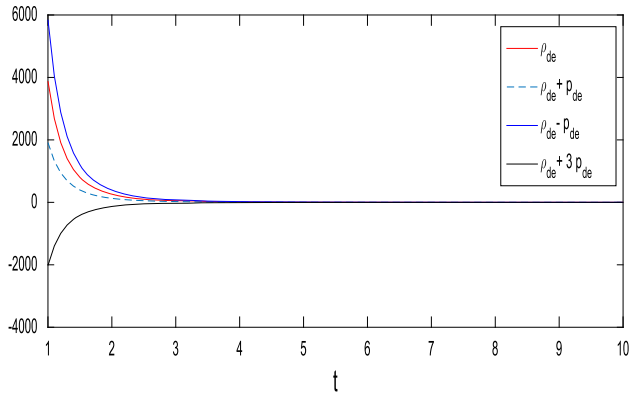

Figure 8. The plot of energy conditions vs. cosmic time t of the interacting model for $\alpha = 1$, $a_1 = 1.5$, $\beta = 0.01$, $k = 0.097$, $m = 1.6$, $\Omega_{m_0} = 0.3$, $\gamma_m = 0$, $M = -0.5$, $X = -1$, $\omega = 1000$ and $\sigma = 0.02$.

The evaluation of the squared speed of sound against cosmic time is shown in figure 9. The graph of c_s^2 in the non-interacting case is similar to that of the interacting model. The present interacting model meets the required bound on c_s^2, i.e. $0 \leq c_s^2 \leq 1$, throughout the cosmic evolution.

5. Anisotropy parameter

The mean anisotropy parameter expansion A_m is defined by

$$A_m = \frac{1}{3}\sum_{i=1}^{3}\left[\frac{\Delta H_i}{H}\right]^2, \tag{51}$$

where $\Delta H_i = H_i - H$ $(i = 1, 2, 3)$ and $H_1 = \dot{A}/A$, $H_2 = \dot{B}/B$ and $H_3 = \dot{C}/C$ are the directional Hubble

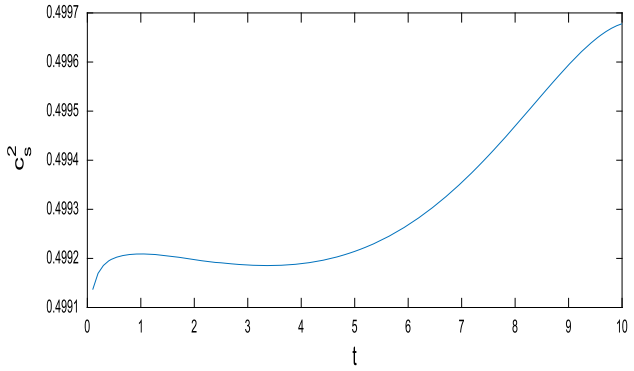

Figure 9. The plot of the squared speed of sound vs. cosmic time t of the interacting model for $\alpha = 1, a_1 = 1.5, \beta = 0.01$, $k = 0.097$, $m = 1.6$, $\Omega_{m_0} = 0.3$, $\gamma_m = 0$, $M = -0.5$, $X = -1$, $\omega = 1000$ and $\sigma = 0.02$.

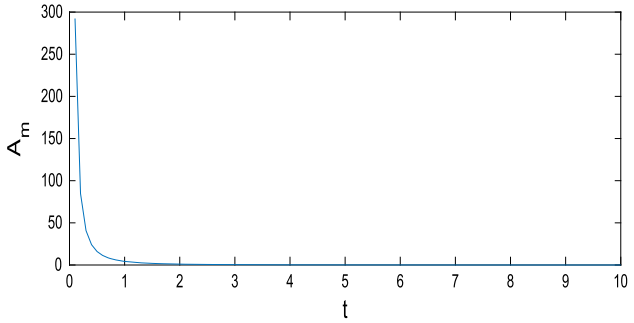

Figure 10. The plot of anisotropy parameter vs. cosmic time t for $\alpha = 1, a_1 = 1.5, \beta = 0.01, k = 0.097, m = 1.6, b_1 = 1$, $b_2 = 0.5$ and $b_3 = 0.3$.

parameters in the directions of x-, y- and z-axes respectively. So, A_m for the considered cosmological model is obtained as

$$A_m = \frac{(b_1^2 + b_2^2 + b_3^2)}{3H^2a^6\phi^2}.$$

Substituting the values of H, a and ϕ in the above equation, we get

$$A_m = \frac{(b_1^2 + b_2^2 + b_3^2)(kt^2 - 2mt)^2}{12\alpha^2\, a_1^{2(\beta+3)} \exp\left(\frac{2(2\beta+6)}{m}\tanh^{-1}\left(\frac{kt}{m} - 1\right)\right)}. \tag{52}$$

Figure 10 exhibits the variation of anisotropy parameter expansion as a function of t. The model shows anisotropic behaviour in nature initially, but as the Universe evolves it approaches isotropy at late times.

6. Statefinder diagnostic

Statefinder diagnostic is a method that was developed [59] to categorise the different DE models. The

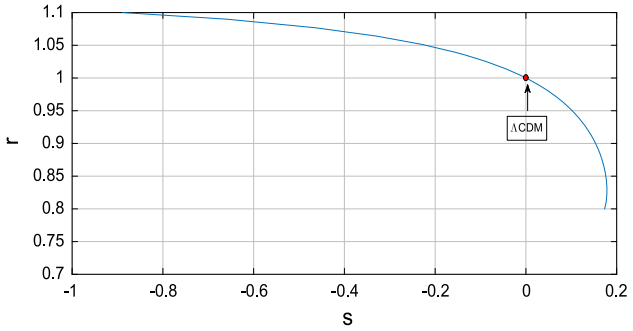

Figure 11. Graph of statefinder diagnostic: r vs. s for $k = 0.097$ and $m = 1.6$.

statefinder parameter diagnostic pair $\{r, s\}$ carries out a systematic inquiry of the Universe's expansion dynamics. The geometrical parameter $\{r, s\}$ is defined as

$$r = \frac{\dddot{a}}{aH^3} \quad \text{and} \quad s = \frac{r-1}{3(q-0.5)}, \quad \text{where } q \neq 0.5.$$

The statefinder diagnostic parameters for the obtained model are given by

$$r = \frac{1}{2}\left[(3kt - 4m + 6)(kt - m) + (kmt + 2)\right],$$
$$s = \frac{\left[(3kt - 4m + 6)(kt - m) + kmt\right]}{6(-kt + m) + 5}.$$

In the r–s plane, trajectories exhibit different behaviour for various DE models. In $\{r, s\}$ diagram, points $(1, 0)$ and $(1, 1)$ are fixed points corresponding to ΛCDM and standard cold dark matter (SCDM) (matter-dominated) models, respectively. Various forms of the DE models such as quintessence, Chaplygin gas, braneworld and some other interacting DE models can be differentiated successfully using statefinder diagnostic analysis. For some particular models, to calculate diverging or converging behaviour of the DE model concerning the SCDM or ΛCDM models, the position of fixed point $\{r, s\}$ can be calculated and located in the diagram. From figure 11, one can observe that initially, the model resembles the behaviour of DE with Chaplygin gas as it evolves in the domain $r > 1, s < 0$. Eventually when time passes, the trajectory enters into quintessence region $(r < 1, s > 0)$ after touching the point $r = 1, s = 0$.

7. Final remarks and conclusion

In this article, we have investigated the non-interacting and interacting DE and DM in the scope of anisotropic Bianchi I Universe in the BD theory of gravity. To determine the exact solution of the field equation, we have considered (i) the power-law relation between the scalar field and cosmic scale factor and (ii) linearly varying deceleration parameter. Firstly, the EoS parameter was calculated in terms of t for both the models. In both cases, from figures 2 and 6, it has been observed that the EoS parameter is a negative valued function that varies in the quintessence regime. More precisely, the Universe is dominated by DE throughout the cosmic evolution in both the cosmological models as the density parameter of DE dominates matter density. Therefore, both the interacting and non-interacting models appear to be realistic. The recent observation [50] suggested that $\Omega \sim 1$, which shows that the Universe is approximately flat as well as infinite. Our model also predicts the flat Universe in the late epoch. We have scrutinised the physical acceptability of the models through energy conditions. The general expressions for standard point-wise conditions are as follows [60–62]:

Null energy condition (NEC): $\Longleftrightarrow \rho_{de} + p_{de} \geq 0$
Weak energy condition (WEC): $\Longleftrightarrow \rho_{de} \geq 0, \rho_{de} + p_{de} \geq 0$
Dominant energy condition (DEC): $\Longleftrightarrow \rho_{de} \geq 0, \rho_{de} \pm p_{de} \geq 0$
Strong energy condition (SEC): $\Longleftrightarrow \rho_{de} + 3p_{de} \geq 0, \rho_{de} + p_{de} \geq 0$

For non-interacting and interacting scenario, $\rho_{de} > 0$, $\rho_{de} \pm p_{de} > 0$ and $\rho_{de} + 3p_{de} < 0$ (as shown in figures 4 and 8) in the initial stage of the Universe but at late times, i.e., as $t \to \infty$, $\rho_{de} \to 0$, $\rho_{de} \pm p_{de} \to 0$ and $\rho_{de} + 3p_{de} \to 0$. Throughout the evolution of the Universe, the non-interacting and interacting models in the framework of the Bianchi I Universe with the BD theory of gravity satisfies WEC and DEC. In contrast, the SEC violates, which fulfills the requirements of the accelerating Universe as per the current observations. The stability of both models was examined by discussing the square sound speed. The obtained cosmological models meet the required bounds of $0 \leq c_s^2 \leq 1$ for the considered free parameter values. Henceforth, the considered cosmological models are stable for considered values of free parameters. Interestingly, the physical parameters, physical acceptability and stability of the non-interacting model resemble the interacting model for $\sigma = 0.02$. The anisotropy parameter of expansion also was calculated and discussed. The model observes anisotropy initially, but as time passes, it tends to isotropy at late times. Statefinder diagnostic was also scrutinised here. Figure 11 illustrates that the obtained model under the composition of BD theory resembles Chaplygin gas and quintessence models during its cosmic evolution.

Acknowledgements

The authors would like to convey appreciation towards the Inter-University Centre for Astronomy and Astrophysics (IUCAA), Pune, India, for providing the facility and hospitality where this work was partially carried out. AL and NH are grateful to Dr Binaya K Bishi for giving some valuable suggestions on the manuscript before submission. The authors would also like to express their sincere thanks to the reviewer and editor for their valuable, constructive suggestions.

References

[1] A G Riess *et al*, *Astron. J.* **116**, 1009 (1998)
[2] S J Perlmutter *et al*, *Astrophys. J.* **517**, 565 (1999)
[3] S J Perlmutter *et al*, *Nature* **391**, 51 (1998).
[4] C L Bennett *et al*, *Astrophys. J. Suppl.* **148**, 1 (2003)
[5] M Tegmark *et al*, *Phys. Rev. D* **69**, 103501 (2004)
[6] C L Bennett *et al*, *Astrophys. J. Suppl.* **148**, 97 (2003)
[7] C L Bennett *et al*, *Astrophys. J.* **583**, 1 (2003)
[8] B Novosyadlyj, O Sergijenko and S Apunevych, *J. Phys. Stud.* **15**, 1901 (2011)
[9] A K Yadav, F Rahaman and S Ray, *Int. J. Theor. Phys.* **50**, 871 (2011)
[10] U Mukhopadhyay, S Ray and F Rahaman, *Int. J. Mod. Phys. D* **19**, 475 (2010)
[11] P P Avelino, L Losano and J J Rodrigues, *Phys. Lett. B* **699**, 10 (2011)
[12] A Burgazli, M Eingorn and A Zhunk, *Eur. Phys. J. C* **75**, 118 (2015)
[13] V Sahni and A Starobinsky, *Int. J. Mod. Phys. D* **15**, 2105 (2006)
[14] N Dalal, K Abazajian, E E Jenkins and A V Manohar, *Phys. Rev. Lett.* **87**, 141302 (2001)
[15] L P Chimento, A S Jakubi and D Pavon, *Phys. Rev. D* **67**, 087302 (2003)
[16] R Bali, *Int. J. Theor. Phys.* **50**, 3043 (2011)
[17] R Bali, *Mod. Phys. Lett. A* **33**, 1850238 (2018)
[18] W F Kao and I Chen Lin, *Eur. Phys. J. C* **77**, 805 (2017)
[19] R Raushan, A K Shukla, R Chaubey and T Singh, *Pramana – J. Phys.* **92**: 5 (2019)
[20] C H Brans and R H Dicke, *Phys. Rev.* **124**, 925 (1961)
[21] S K Rama and S Ghosh, *Phys. Lett. B* **383**, 31 (1966)
[22] S K Rama, *Phys. Lett. B* **373**, 282 (1966)
[23] C Romero and A Barros, *Phys. Lett. A* **173**, 243 (1993)
[24] N Banerjee and D Pavon, *Phys. Rev. D* **63**, 043504 (1966)
[25] A Chand, R K Mishra and A Pradhan, *Astrophys. Space Sci.* **361**, 81 (2016)
[26] G P Singh, A Y Kale and J Tripathi, *Rom. J. Phys.* **58**, 23 (2013)
[27] G P Singh and B K Bishi, *Adv. High Energy Phys.* **1390572**, 2017 (2017)
[28] T Singh and L N Rai, *Gen. Rel. Grav.* **15**, 875 (1983)
[29] H Amirhashchi, A Pradhan and H Zainuddin, *Res. Astron. Astrophys.* **13**, 129 (2013)
[30] H Amirhashchi, *Res. Astron. Astrophys.* **14**, 1121 (2014)
[31] K S Adhav, S L Munde, G B Tayade and V D Bokey, *Astrophys. Space Sci.* **359**, 24 (2015)
[32] H Amirhashchi, S N Ali Qazi and H Zainuddin, *Res. Astron. Astrophys.* **14**, 1383 (2014)
[33] J E Gonzalez, H H B Silva, R Silva and J S Alcaniz, *Eur. Phys. J. C* **78**, 730 (2018)
[34] N Tamanini, *Phys. Rev. D* **92**, 043524 (2015)
[35] G K Goswami, A Pradhan and A Beesham, *Pramana – J. Phys.* **93**: 89 (2019)
[36] H Amirhashchi, A Pradhan and R Jaiswal, *Int. J. Theor. Phys.* **52**, 2735 (2013)
[37] B Saha, H Amirhashchi and A Pradhan, *Astrophys. Space Sci.* **342**, 257 (2012)
[38] H Amirhashchi, D S Chouhan and A Pradhan, *Electron. J. Theor. Phys.* **11**, 109 (2014)
[39] S D Katore and D V Kapse, *Adv. High Energy Phys.* **2854567**, 2018 (2018)
[40] M F Shamir and A A Bhatti, *Can. J. Phys.* **90**, 193 (2012)
[41] A Barros and C Romero, *Mod. Phys. Lett. A* **18**, 2117 (2003)
[42] V B Johri and K Desikan, *Gen. Rel. Grav.* **26**, 1217 (1994)
[43] D K Ciftci and V Faraoni, *Ann. Phys.* **391**, 65 (2018)
[44] O Akarsu and T Dereli, *Int. J. Theor. Phys.* **51**, 612 (2012)
[45] A G Riess *et al*, *Astrophys. J.* **607**, 665 (2004)
[46] J V Cunha and J A S Lima, *Mon. Not. R. Astron. Soc.* **390**, 210 (2008)
[47] J V Cunha, *Phys. Rev. D* **79**, 047301 (2009)
[48] R Nair, S Jhingan and D Jain, *J. Cosmol. Astropart. Phys.* **1201**, 018 (2012)
[49] O Akarsu, S Kumar, R Myrzakulov, M Sami and L Xu, *J. Cosmol. Astropart. Phys.* **1401**, 022 (2014)
[50] N Aghanim *et al*, arXiv:1807.06209 [astro-ph.CO] (2018)
[51] R Chaubey and A K Shukla, *Pramana – J. Phys.* **88**: 65 (2017)
[52] F Wu and X Chen, *Phys. Rev. D* **82**, 083003 (2010)
[53] A G Riess *et al*, *Astrophys. J* **699**, 539 (2009)
[54] L Xu, J Lu and W Li, arXiv:0905.4174 [astro-ph.CO] (2009)
[55] V Acquaviva, C Baccigalupi, S M Leach, A R Liddle and F Perrotta, *Phys. Rev. D* **71**, 104025 (2005)
[56] I Quiros *et al*, *Class. Quant. Grav.* **35**, 075005 (2018)
[57] Z K Guo, N Ohta and S Tsujikawa, *Phys. Rev. D* **76**, 023508 (2007)
[58] D Pavon and B wang, *Gen. Rel. Grav.* **41**, 1 (2009)
[59] V Sahni, T D Saini, A A Starobinsky and U Alam, *JETP Lett.* **77**, 201 (2003)
[60] S W Hawking and G F R Ellis, *The large-scale structure of space-time* (Cambridge University Press, Cambridge, 1973)
[61] R M Wald, *General relativity* (University of Chicago Press, Chicago, 1984
[62] M Visser, *Science* **276**, 88 (1997)